

CHEMISTRY

AN ASIAN JOURNAL

www.chemasianj.org

Accepted Article

Title: Multiplexed Metabolic Labeling of Glycoconjugates in Polarized Primary Cerebral Cortical Neurons

Authors: Ji Yu Choi, Jeongyeon Seo, Matthew Park, Mi-Hee Kim, Kyungtae Kang, and Insung S. Choi

This manuscript has been accepted after peer review and appears as an Accepted Article online prior to editing, proofing, and formal publication of the final Version of Record (VoR). This work is currently citable by using the Digital Object Identifier (DOI) given below. The VoR will be published online in Early View as soon as possible and may be different to this Accepted Article as a result of editing. Readers should obtain the VoR from the journal website shown below when it is published to ensure accuracy of information. The authors are responsible for the content of this Accepted Article.

To be cited as: *Chem. Asian J.* 10.1002/asia.201800996

Link to VoR: <http://dx.doi.org/10.1002/asia.201800996>

A Journal of



A sister journal of *Angewandte Chemie*
and *Chemistry – A European Journal*

WILEY-VCH

COMMUNICATION

Multiplexed Metabolic Labeling of Glycoconjugates in Polarized Primary Cerebral Cortical Neurons

Ji Yu Choi,^[a] Jeongyeon Seo,^[a] Matthew Park,^[a] Mi-Hee Kim,^[a] Kyungtae Kang,^{*[b]} and Insung S. Choi^{*[a]}

Abstract: The spatial distribution of cell-surface glycoconjugates in the brain changes continuously, reflecting neurophysiology especially in the developing phase, but their functions and fates mostly remain unexplored. Their spatiotemporal distribution is particularly important in the polarized neuronal cells, such as cerebral cortical neurons composed of a soma and neurites. In this work, we dually labeled sialic acid (Sia5Ac) and *N*-acetylgalactosamine/glucosamine (GalNAc/GlcNAc) by a neurocompatible strategy of metabolic glycan labeling, metabolism-by-tissues (MbT), and obtained the multiplexed information on their spatiotemporal distribution on the polarized cortical neurons. The analyses showed the preferentially distinct distribution of each saccharide set at the late developmental stage after randomized, heterogeneous distribution at the early stage, suggesting Sia5Ac and GalNAc/GlcNAc are translocated anisotropically during neuronal development.

Glycoconjugates in cortical neurons regulate many basal functions of neurons including migration, neuritogenesis, neurite outgrowth, synapse formation, and synaptic efficacy,^[1] as they do in other cell types.^[2] With sophisticated orchestration at the tissue level do they direct the migration and subsequent differentiation of cortical neurons simultaneously,^[3] which collectively dictate the formation of the well-organized, six-layered laminar structure of a cerebral cortex—a brain area (also called brain stem) responsible for sensory recognition, movement execution, consciousness, and memory.^[4] TAG-1—a glycosylphosphatidylinositol-linked glycoprotein mainly expressed on tangentially migrating neurons in the cortex—controls neuronal adhesion and migration,^[5] and GM2 [GalNAc β 1-4(NeuAc α 2-3)Gal β 1-4Glc β 1-1Cer, a subtype of sialylated glycosphingolipids] ganglioside regulates dendritogenesis in a developing cortex^[6] or cultured cortical pyramidal neurons.^[7] Furthermore, glycans dynamically regulate the functions of biomolecules according to biological context, as shown in the cases of polysialic acid on neural cell adhesion molecule (NCAM),^[8] *N*-acetylgalactosamine (GalNAc) on Tn antigen,^[9] and *N*-acetylglucosamine (GlcNAc) on synapsin I.^[10] Despite of the consistent (and often critical) presence of glycoconjugates in cells, molecular-level analysis and understanding of their functions have been challenging, primarily because glycoconjugates are extremely heterogeneous in form

(e.g., multiple subtypes of gangliosides, such as GM1, GD1a, GD1b, and GT1b^[11]), and their structures and functions are intractable with the conventional bioanalytical methods such as electrophoresis and mass spectroscopy. In this respect, the method of metabolic glycan labeling has emerged as an elegant and powerful tool in glycochemistry,^[12] which has intensively been used to visualize the spatiotemporal distribution of monosaccharides,^[13] to enrich glycoproteins or glycolipids for mass spectroscopic analysis,^[14] and even to identify certain cells.^[15] Although the method has advanced to label specific glycans, such as *N*-linked glycans or *O*-linked GlcNAc with proper modification of metabolic probes,^[16] most work has so far been limited to the membrane-wide, generalized imaging of surface glycans. That is, the studies on their localized distribution in a cell membrane have been lacking, which are important particularly for anisotropic, polarized neurons. The neuron is typically distinguished by its large surface area of about 250,000 μm^2 (as a comparison, about 1,256 μm^2 for isotropic, spherical cells with a diameter of 20 μm)^[17], and, more importantly, consists of morphologically distinct membrane domains, such as a soma, neurites (morphological part), a presynapse on the axon and a postsynapse on the dendrite (functional part). Therefore, the information on the relative spatial-distribution of glycoconjugates in the polarized neurons would be highly beneficial in neuroglycomics and neural physiology.

The application of metabolic glycan labeling to neurons has been challenging because of the apparent neurotoxicity of unnatural monosaccharide precursors (e.g., *N*-glycolylmannosamine pentaacetate and peracetylated *N*-azidoacetyl-D-mannosamine (Ac₄ManNAz)).^[18-20] In this work, we utilized a recently developed strategy for neurocompatible metabolic glycan labeling of primary cortical neurons (metabolism-by-tissues, MbT, Figure 1)^[19] to acquire multiplexed information on the spatiotemporal distribution of two different glycoconjugates—one with sialic acid (Sia5Ac) and the other with *N*-acetylgalactosamine/glucosamine (GalNAc/GlcNAc). Specifically, we simultaneously fed a cortical tissue (before dissociation into cortical neurons) with two different unnatural monosaccharides: peracetylated *N*-(4-pentynoyl)-D-mannosamine (Ac₄ManNAI) as a Sia5Ac precursor and peracetylated *N*-azidoacetyl-D-galactosamine (Ac₄GalNAz) as a metabolic precursor of GalNAc/GlcNAc. The acetyl (Ac) groups of Ac₄ManNAI and Ac₄GalNAz facilitate their passing through the cell membrane via diffusion and are subsequently hydrolyzed by cytosolic esterases in the cytosol. The deprotected Ac₄ManNAI, ManNAI, is phosphorylated and transformed to a Sia5Ac analogue by *N*-acetylmannosamine kinase, sialic acid 9-phosphate synthase, and sialic acid 9-phosphatase. For the sialylation, the analogue is subsequently activated with cytidine monophosphate (CMP) in the nucleus and transported into the Golgi compartment. On the other hand, deacetylated Ac₄GalNAz, GalNAz, is phosphorylated and activated with uridine diphosphate

[a] J. Y. Choi, J. Seo, Dr. M. Park, Dr. M.-H. Kim, Prof. Dr. I. S. Choi
Center for Cell-Encapsulation Research
Department of Chemistry
KAIST, Daejeon 34141, Korea
E-mail: ischoi@kaist.ac.kr

[b] Prof. Dr. K. Kang
Department of Applied Chemistry
Kyung Hee University
Yongin, Gyeonggi 17104, Korea

Supporting information for this article is given via a link at the end of the document.

COMMUNICATION

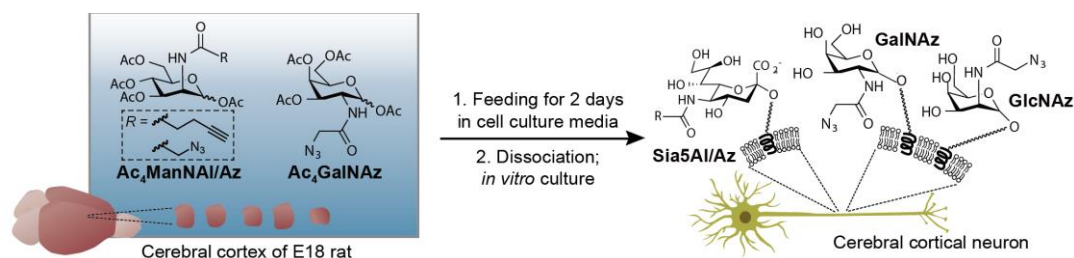


Figure 1. Schematic illustration for the neurocompatible labeling of cortical-neuron glycans. Unnatural monosaccharide precursors were incorporated to primary cortical neurons at the tissue level, and the cortical tissue were dissociated into individual neuron cells.

(UDP) in the cytosol, and some but not all UDP-GalNAz are transformed into UDP-GlcNAz by UDP-galactose 4-epimerase.^[14,21] Thus, in the primary cerebral cortical neuron, both UDP-GalNAz/GlcNAz are generated, transported to the Golgi lumen, and utilized for glycosylation of lipids and proteins. According to these salvage pathways, we used two chemically orthogonal alkynyl precursor-Ac₄ManNAI and azido precursor-Ac₄GalNAz for the multiplexed imaging of Sia5Ac- and GalNAc/GlcNAc-glycoconjugates.

The experimental conclusion that the conventional method for metabolic glycan labeling—involving the feeding of dissociated cells with unnatural monosaccharides^[22]—was inapplicable to primary cerebral cortical neurons was made, in this work, with three peracetylated unnatural monosaccharides, Ac₄GalNAz, Ac₄ManNAI, and Ac₄ManNAz. Ac₄ManNAz was additionally examined for neurotoxicity studies, because it had been used most intensively for metabolic glycan labeling in the previous reports and considered as a neurotoxic probe.^[19] As shown in Figure 2, the viability of the cortical neurons decreased gradually over time, when they were fed with Ac₄ManNAz, Ac₄ManNAI or Ac₄GalNAz (50 μM) under the conventional protocol (see the Supporting Information for the experimental details). For example, the relative viability of Ac₄ManNAz- or Ac₄GalNAz-fed cortical neurons to non-treated cells as a reference was 5.5% or 12.0% at 4 DIV (DIV: days *in vitro*) (Figures 2a and b). Although Ac₄ManNAI was less neurotoxic (79.2% at 4 DIV) than Ac₄ManNAz and Ac₄GalNAz, the longest neurite length (119.7 ± 4.3 μm at 4 DIV) was much shorter than that of the control reference (264.0 ± 12.0 μm, Figures 2c and S1). As related work, Yarema and co-workers have studied the metabolic flux of ManNAc analogues and their effects on cellular activities, viability, and growth, and reported that the extremely high dose of Ac₄ManNAz (300 μM) increased the caspase activity and induced the apoptosis of Jurkat cells.^[23] In comparison, our work showed that even low dose (50 μM) was lethal to primary cortical neurons, necessitating the development of alternative strategies for metabolic glycan labeling of the neurons.

In a stark contrast with the conventional method, the MbT method proved highly compatible with primary cortical neurons. In the MbT method, briefly, cerebral cortical tissues were dissected from E18 Sprague-Dawley rat pups, sliced into pieces, and incubated with a metabolic precursor (50 μM). After two days of feeding, the tissues were dissociated to individual cells prior to seeding (0 DIV). The results indicated that the viability of cortical neurons under the MbT method was comparable to or even slightly higher than that of the reference (Figures 3a and b), confirming the validity of the MbT method for metabolic glycan labeling of primary cortical

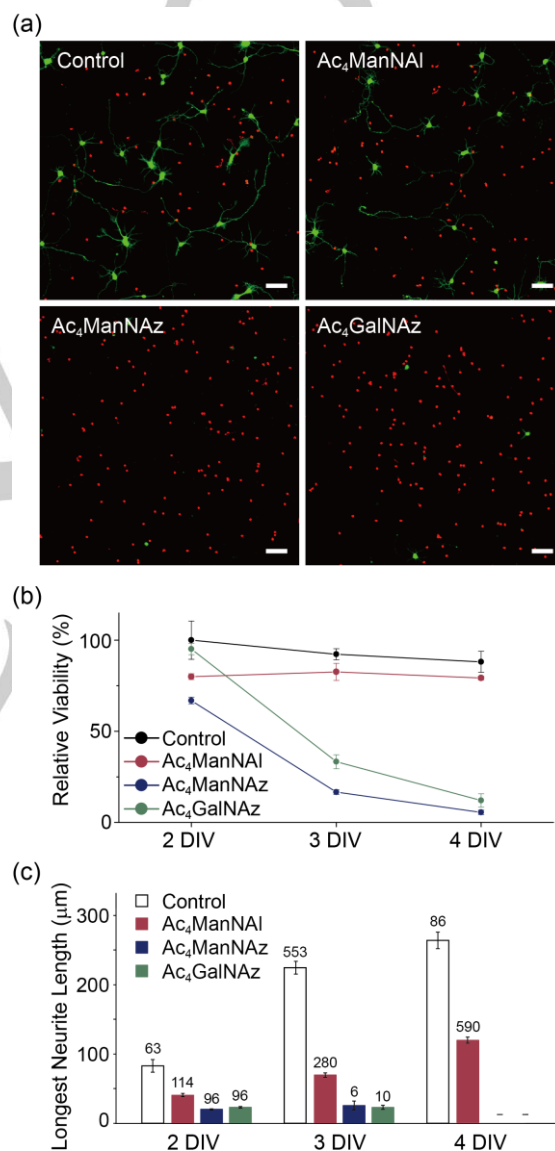


Figure 2. Neurotoxicity of unnatural monosaccharides in the conventional method. (a) Confocal laser-scanning microscopy (CLSM) images of primary cortical neurons at 4 DIV after staining with a live-dead assay kit (green: live; red: dead). The scale bars are 50 μm. (b) Relative viabilities of the neurons modified with unnatural monosaccharides to non-treated cortical neurons as a reference in conventional method. Relative viability (%): the viability of the precursor-treated cortical neurons divided by the viability of the non-treated cortical neurons (in %, mean ± S.E). The experiments were performed in triplicate. Control: non-treated cortical neurons. (c) Averaged longest-neurite length of neurons at 2, 3, and 4 DIV (mean ± S.E). The numbers on the bars indicate the number of cells analyzed.

For internal use, please do not delete. Submitted_Manuscript

COMMUNICATION

neurons. For example, the relative viability of the Ac₄ManNAI-fed neurons was about 99% at 1 DIV, and the value was 110% for the Ac₄GalNAz-fed ones at 1 DIV. In addition, under the MbT method, the unnatural monosaccharides did not disturb neurite outgrowth and elongation; the averaged longest neurite lengths of the single neurons (except for the cells connected to neighborhood ones) were $54.0 \pm 3.4 \mu\text{m}$ for the control reference, $54.1 \pm 5.0 \mu\text{m}$ for Ac₄ManNAI, and $48.0 \pm 3.1 \mu\text{m}$ Ac₄GalNAz at 2 DIV (Figures 3c and S1). After confirming the neurocompatibility of the MbT method with primary cortical neurons, we investigated the metabolic incorporation of Ac₄ManNAz, Ac₄ManNAI, and Ac₄GalNAz by bioorthogonal copper-catalyzed azide-alkyne cycloaddition (CuAAC) with a green-fluorescent dye (Alexa Fluor® 488-azide or -alkyne) at 1 DIV. The CLSM images confirmed that all the three unnatural precursors were successfully metabolized and incorporated to the cortical neurons (Figures S2 and S3).

We envisioned that GalNAc/GlcNAc and Sia5Ac would have distinct cellular distribution patterns in the polarized cortical neurons, reflecting constantly varying physiological state of the cells, and thus, we investigated their time-dependent distributions by two-color labeling at different time points. Both Ac₄ManNAI and Ac₄GalNAz were fed simultaneously to the cortical slices, by taking advantage of the chemical orthogonality of CuAAC, for the dual labeling. The cytotoxicity test confirmed that the combined administration of Ac₄ManNAI (50 μM) and Ac₄GalNAz (50 μM) did not alter neuronal survival and neurite outgrowth, including development of axons and dendrites (Figures S4 and S5). After dissociation and culture, the chemo-metabolically incorporated Sia5AI and GalNAz/GlcNAz on the cell surfaces were reacted orthogonally with alkyne-linked, green Alexa Fluor® 488 (Alexa 488-AI) and azide-linked, red Alexa Fluor® 594 (Alexa 594-Az), respectively, at 1, 2, and 8 DIV. As seen in Figures 4a and S6, at the early developmental stage (2 DIV), the spatial distribution of Sia5AI and GalNAz/GlcNAz was neither distinct and nor distinguishable, and, additionally, was inconsistent among the cells, implying heterogeneous character of initial neuronal development. For example, some neurons showed a dominant distribution of Sia5AI over GalNAz/GlcNAz, while others exhibited the opposite or equal distributions. Localized distribution at somas and neurites was also heterogeneous among cells. Accordingly, further statistical analysis of the early-stage distribution was conducted at the single-cell level. The mean fluorescence intensities of green (for GalNAz/GlcNAz) and red (for Sia5AI) (mean fluorescence intensity = total fluorescence intensity of a cell divided by the cell area) were calculated for each neuron at 1 DIV, and their distributions were plotted as blue dots on the 2D coordinate of green (*x*-axis) and red fluorescence (*y*-axis) (Figure S7). The same analysis was also performed at 2 DIV and displayed with orange dots in the scatterplot to investigate the time-dependent evolution of GalNAz/GlcNAz and Sia5AI in the relative sense. Overall, the scatterplot showed lower green intensity at 2 DIV (orange dots) than 1 DIV (blue dots). For the statistical analysis, the averaged mean fluorescence intensity was calculated for the green fluorescence (Alexa 488 AI-conjugated GalNAz/GlcNAz). The value was found to be statistically lower at 2 DIV than that measured at 1 DIV (8.59 ± 0.20 at 1 DIV and 6.67 ± 0.15 at 2 DIV, $p < 0.0001$), implying that the labeled GalNAc/GlcNAc might return to the cytosol between 1 DIV and 2 DIV and be replaced with natural, non-fluorescent

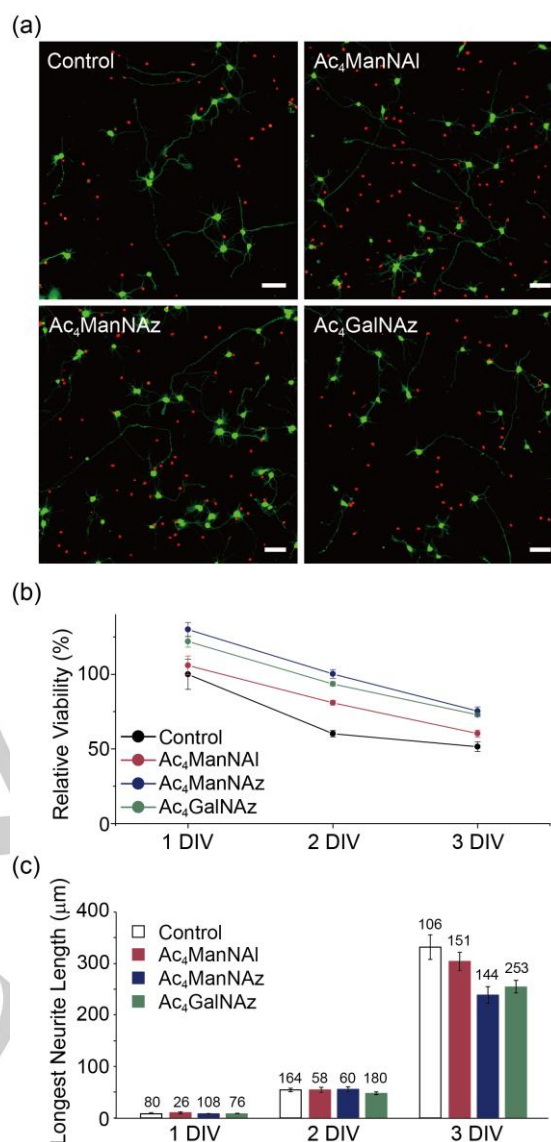


Figure 3. Mitigation of neurotoxicity of unnatural monosaccharides by using MbT method. (a) CLSM images of primary cortical neurons at 3 DIV after staining with a live-dead assay kit (green: live; red: dead). The scale bars are 50 μm . (b and c) Neurocompatibility of the MbT method: (b) Relative viabilities of neurons modified with unnatural monosaccharides to non-treated cortical neurons as a reference in MbT method. Relative viability (%): the viability of the precursor-treated cortical neurons divided by the viability of the non-treated cortical neurons (in %, mean \pm S.E). The experiments were performed in triplicate. Control: non-treated cortical neurons. (c) Averaged longest-neurite length at 1, 2, and 3 DIV (mean \pm S.E). The numbers on the bars indicate the number of cells analyzed.

GalNAc/GlcNAc. The statistical insignificance found for the red fluorescence suggested that the recycling/turnover rate of Sia5Ac would be slower than that of GalNAc/GlcNAc during the first two days of culture. We further analyzed the fluorescence data by calculating the ratio of red-to-green fluorescence per neuron, and did not observe statistically significant difference between 1 and 2 DIV (0.51 ± 0.03 at 1 DIV and 0.67 ± 0.07 at 2 DIV, $p < 0.05$) (Figure 4b). However, when the calculated ratios were grouped into three ranges—0-0.5, 0.5-1, and >1 , more neurons were classified to the range of >1 and less to the range of 0-0.5 at 2 DIV, further implying that the turnover of GalNAc/GlcNAc was relatively faster than Sia5Ac (Figure 4b).

For internal use, please do not delete. Submitted_Manuscript

COMMUNICATION

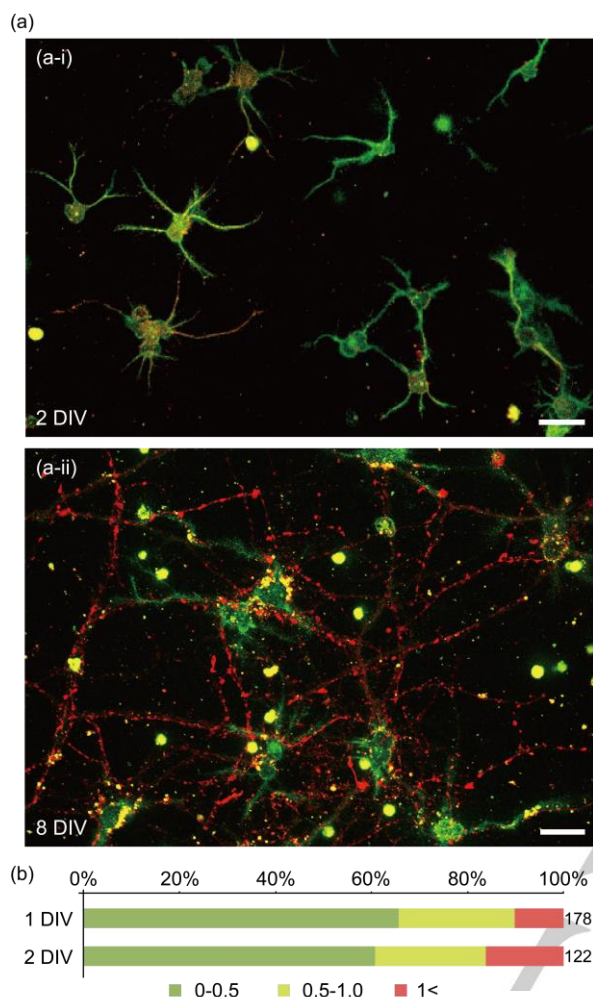


Figure 4. (a) CLSM images of two-color labeled cortical neurons at (i) 2 and (ii) 8 DIV. The scale bars are 25 μ m. (b) Distributions of the red-to-green ratios at 1 and 2 DIV. The ratios were divided into the ranges of 0-0.5, 0.5-1.0, and >1. The numbers on the bars indicate the number of cells analyzed.

At the later stage of development, the preferential spatial distribution of GalNAz/GlcNAz and Sia5AI in the highly polarized cortical neurons was clearly discernable (8 DIV, Figure 4a-ii). The CLSM images clearly showed that red-fluorescent Sia5AI were more observable at the neurites, while the presence of green-fluorescent GalNAz/GlcNAz was dominant near the soma (Figure 4a-ii). This observation was intriguing, because it indicated that the fate of surface glycans (e.g., turnover and relocation) was not random but rather controlled tightly in the directionality with the polarized cell. That is, in the case of developing cortical neurons, glycans with GalNAz/GlcNAz stayed at and near soma during neurite outgrowth, but glycans with Sia5AI were relocated to the growing neurites. Taken all together, our results suggested that glycoconjugates were distributed randomly on the cell membrane at the early phase of development (when the cell was rather isotropic), and their preferential distribution and relocation occurred at the later stage of neuronal development when the neuron became highly polarized. In developing cerebral cortex of mice, from an embryo to the adult, the expression of glycans and glycoproteins—*N*-linked glycans including Lewis X antigens and more than 140 glycosyltransferases and glycosidases—were reported to be remarkably changed.^[24] Thus, the relocation of

glycoconjugates on the membrane, as seen in Figure 4, might be a beginning step or a part of drastic alterations of glycans in the brain development.

Biological information carried by cell-surface glycans is of utmost importance to understand the dynamic aspects of neuronal networks (e.g., neuronal development, axon guidance, synaptic plasticity, and neuron-glia interaction), but the surface glycans in neurons have not been studied to the extent that such information could be gathered and deciphered. In this work, we performed orthogonal two-color labeling of GalNAz/GlcNAz and Sia5Ac on the surface of polarized cortical neurons via neuro-compatible MbT method, and showed that each glycoconjugate set exhibited distinct and localized spatial distribution on the cell surface. In addition, each set of saccharides had its own dynamics of turnover and relocation at the later stage of neuronal development, while there was only randomized spreading of glycans at the early stage. We believe that our work would suggest a simple but powerful means to study preferential distribution of surface glycans in the neuronal cells, and related future work would further provide valuable information regarding the translocation of various surface glycoconjugates and their unknown biochemical roles.

Acknowledgements

This work was supported by the Basic Science Research Program through the National Research Foundation of Korea (NRF) funded by the Ministry of Science, ICT & Future Planning (MSIP) (2012R1A3A2026403) and the GRRC program of Gyeonggi province [GRRC-kyunghee2018(A01)].

Conflict of interest

The authors declare no conflict of interest.

Keywords: Glycoconjugates • Metabolic glycan labeling • Metabolism-by-tissues • Neurocompatibility

- [1] a) R. Kleene, M. Schachner, *Nat. Rev. Neurosci.* **2004**, *5*, 195–208; b) H. E. Murrey, L. C. Hsieh-Wilson, *Chem. Rev.* **2008**, *108*, 1708–1731.
- [2] a) H. Ghazarian, B. Idoni, S. B. Oppenheimer, *Acta Histochem.* **2011**, *113*, 236–247; b) L. L. Kiessling, R. A. Splain, *Annu. Rev. Biochem.* **2010**, *79*, 619–653.
- [3] a) B. Nadarajah, J. G. Parnavelas, *Nat. Rev. Neurosci.* **2002**, *3*, 423–432; b) M. Denaxa, K. Kyriakopoulou, K. Theodorakis, G. Trichas, M. Vidaki, Y. Takeda, K. Watanabe, D. Karagogeos, *Dev. Biol.* **2005**, *288*, 87–99.
- [4] a) B. J. Molyneaux, P. Arlotta, J. R. L. Menezes, J. D. Macklis, *Nat. Rev. Neurosci.* **2007**, *8*, 427–437; b) L. W. Swanson, *Trends Neurosci.* **1995**, *18*, 471–474.
- [5] D. P. Wolfer, A. Henehan-Beatty, E. T. Stoekli, P. Sonderegger, H.-P. Lipp, *J. Comp. Neurol.* **1994**, *345*, 1–32.
- [6] L. A. Goodman, S. U. Walkley, *Dev. Brain Res.* **1996**, *31*, 162–171.
- [7] S. U. Walkley, D. A. Siegel, K. Dobrenis, *Neurochem. Res.* **1995**, *20*, 1287–1299.
- [8] a) U. Rutishauser, *J. Cell. Biochem.* **1998**, *70*, 304–312; b) A. Acheson, J. L. Sunshine, U. Rutishauser, *J. Cell. Biol.* **1991**, *114*, 143–153.
- [9] K. Akita, S. Fushiki, T. Fujimoto, M. Inoue, K. Oguri, M. Okayama, I. Yamashina, H. Nakada, *J. Neurosci. Res.* **2001**, *65*, 595–603.

For internal use, please do not delete. Submitted_Manuscript

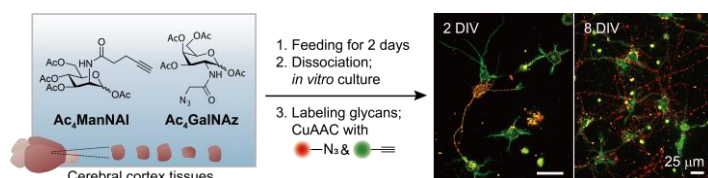
COMMUNICATION

- [10] Y. Skorobogatko, A. Landicho, R. J. Chalkley, A. V. Kossenkov, G. Gallo, and K. Vosseller, *J. Biol. Chem.* **2014**, *289*, 3602-3612.
- [11] K. Vajn, B. Viljetić, I.V. Degmečić, R. L. Schnaar, M. Heffer, *PLoS One* **2013**, *8*, e75720.
- [12] L. K. Mahal, K. J. Yarema, C. R. Bertozzi, *Science* **1997**, *276*, 1125-1128.
- [13] a) S. T. Laughlin, J. M. Baskin, S. L. Amacher, C. R. Bertozzi, *Science* **2008**, *320*, 664-667; b) H. Jiang, B. P. English, R. B. Hazan, P. Wu, B. Ovryn, *Angew. Chem. Int. Ed.* **2015**, *54*, 1765-1769.
- [14] C. M. Woo, A. T. Iavarone, D. R. Spiciarich, K. K. Palaniappan, C. R. Bertozzi, *Nat. Methods* **2015**, *12*, 561-567.
- [15] H. Wang, R. Wang, K. Cai, H. He, Y. Liu, J. Yen, Z. Wang, M. Xu, Y. Sun, X. Zhou, Q. Yin, L. Tang, I. T. Dobrucki, L. W. Dobrucki, E. J. Chaney, S. A. Boppart, T. M. Fan, S. Lezmi, X. Chen, L. Yin, J. Cheng, *Nat. Chem. Biol.* **2017**, *13*, 415-424.
- [16] a) Y. Zhu, J. Wu, X. Chen, *Angew. Chem. Int. Ed.* **2016**, *55*, 9301-9305; b) B. W. Zaro, A. R. Batt, K. N. Chuh, M. X. Navarro, M. R. Pratt, *ACS Chem. Biol.* **2017**, *12*, 787-794.
- [17] K. H. Pfenninger, *Nat. Rev. Neurosci.* **2009**, *10*, 251-261.
- [18] B. E. Collins, T. J. Fralich, S. Itonori, Y. Ichikawa, R. L. Schnaar, *Glycobiology* **2000**, *10*, 11-20.
- [19] K. Kang, S. Joo, J. Y. Choi, S. Geum, S.-P. Hong, S.-Y. Lee, Y. H. Kim, S.-M. Kim, M.-H. Yoon, Y. Nam, K.-B. Lee, H.-Y. Lee, I. S. Choi, *Proc. Natl. Acad. Sci. USA* **2015**, *112*, E241-E248.
- [20] J. Y. Choi, M. Park, H. Cho, M.-H. Kim, K. Kang, I. S. Choi, *ACS Chem. Neurosci.* **2017**, *8*, 2607-2612.
- [21] M. Boyce, I. S. Carrico, A. S. Ganguli, S.-H. Yu, M. J. Hangauer, S. C. Hubbard, J. J. Kohler, and C. R. Bertozzi, *Proc. Natl. Acad. Sci. USA* **2011**, *108*, 3141-3146.
- [22] a) E. Saxon, C. R. Bertozzi, *Science* **2000**, *287*, 2007-2010; b) J. M. Baskin, J. A. Prescher, S. T. Laughlin, N. J. Agard, P. V. Chang, I. A. Miller, A. Lo, J. A. Codelli, C. R. Bertozzi, *Proc. Natl. Acad. Sci. USA* **2007**, *104*, 16793-16797.
- [23] a) E. J. Kim, S.-G. Sampathkumar, M. B. Jones, J. K. Rhee, G. Baskaran, S. Goon, K. J. Yarema, *J. Biol. Chem.* **2004**, *279*, 18342-18352; b) R. T. Almaraz, U. Aich, H. S. Khanna, E. Tan, R. Bhattacharya, S. Shah, K. J. Yarema, *Biotechnol. Bioeng.* **2012**, *109*, 992-1006.
- [24] A. Ishii, T. Ikeda, S. Hitoshi, I. Fujimoto, T. Torii, K. Sakuma, S. Nakakita, S. Hase, K. Ikenaka, *Glycobiology* **2007**, *17*, 261-267.

COMMUNICATION

Entry for the Table of Contents

COMMUNICATION



Ji Yu Choi, Jeongyeon Seo, Matthew Park, Mi-Hee Kim, Kyungtae Kang,*
Insung S. Choi*

Page No. – Page No.

**Multiplexed Metabolic Labeling of
Glycoconjugates in Polarized Primary
Cerebral Cortical Neurons**

Simultaneous metabolic labeling of sialic acid and *N*-acetylgalactosamine/glucosamine glycans in primary cortical neurons via a neurocompatible strategy of MbT (metabolism-by-tissues) showed the glycoconjugate-specific spatial distributions at the late developmental stage (8 DIV) after randomized, heterogeneous distribution at the early stage (2 DIV).